© 2021. Published by The Company of Biologists Ltd | Journal of Experimental Biology (2021) 224, jeb242364. doi:10.1242/jeb.242364

RESEARCH ARTICLE

Rapid embryonic development supports the early onset of gill functions in two coral reef damselfishes

Leteisha A. Prescott[1,2,*], Amy M. Regish[3], Shannon J. McMahon[1], Stephen D. McCormick[3,4] and Jodie L. Rummer[1,2]

ABSTRACT

The gill is one of the most important organs for growth and survival of fishes. Early life stages in coral reef fishes often exhibit extreme physiological and demographic characteristics that are linked to well-established respiratory and ionoregulatory processes. However, gill development and function in coral reef fishes is not well understood. Therefore, we investigated gill morphology, oxygen uptake and ionoregulatory systems throughout embryogenesis in two coral reef damselfishes, *Acanthochromis polyacanthus* and *Amphiprion melanopus* (Pomacentridae). In both species, we found key gill structures to develop rapidly early in the embryonic phase. Ionoregulatory cells appear on gill filaments 3–4 days post-fertilization and increase in density, whilst disappearing or shrinking in cutaneous locations. Primary respiratory tissue (lamellae) appears 5–7 days post-fertilization, coinciding with a peak in oxygen uptake rates of the developing embryos. Oxygen uptake was unaffected by phenylhydrazine across all ages (pre-hatching), indicating that haemoglobin is not yet required for oxygen uptake. This suggests that gills have limited contribution to respiratory functions during embryonic development, at least until hatching. Rapid gill development in damselfishes, when compared with that in most previously investigated fishes, may reflect preparations for a high-performance, challenging lifestyle on tropical reefs, but may also make reef fishes more vulnerable to anthropogenic stressors.

KEY WORDS: Ionoregulatory hypothesis, Oxygen hypothesis, Gas exchange, Metabolic rate, Ionocytes, Ontogeny

INTRODUCTION

Gill formation is an essential process in the early developmental stages of many aquatic organisms including fish, for which the gills are the primary site for vital physiological processes, including oxygen (O_2) uptake, iono/osmoregulation, acid–base regulation and ammonia excretion (Evans et al., 2005). Gills also provide a secondary site for hormonal control, immune defence and food capture (Evans, 1998). It is therefore surprising that, for teleost fishes, the structure and function of gills during early life stages are relatively understudied when compared with adult life stages. As far back as the 1980s, studies started exploring the onset of gill function at early life stages (Burggren and Pinder, 1991; Rombough, 1988; Kimmel et al., 1995) and the external and internal drivers of gill formation during development (Brauner and Rombough, 2012; Rombough, 2007; Baker et al., 2015; Rombough, 2002; Fu et al., 2010; Rombough and Drader, 2009; Rombough, 1999, 1998). These efforts are already showing applied importance in conservation biology, where exposure to environmental stressors – during any life stage – can lead to impairment of gill structure and function (Hess et al., 2017, 2015; Berry et al., 2016). However, our understanding of gill formation and its developmental significance across teleost fishes is still emerging.

Currently, there are two hypotheses explaining the first function of the developing teleost gill. The first, proposed by Krogh (1941), suggests that gills develop to meet the O_2 demands of a developing fish (Krogh, 1941). During early development, fish embryos and larvae absorb O_2 across the skin and yolk-sac epithelium directly into the tissues or the plasma (Feder and Burggren, 1985). However, this mode of O_2 uptake becomes less sustainable as the surface area to volume ratio (SA/V) of embryos declines with growth (Rombough and Moroz, 1997). Thus, the oxygen hypothesis argues that limitations to O_2 uptake through cutaneous pathways necessitates gill development (reviewed in Rombough, 2007). The second hypothesis is the ionoregulatory hypothesis, which suggests that the first function of fish gills is for ion transport to achieve acid–base, ion, water and ammonia regulation (reviewed by Rombough, 2007; Brauner and Rombough, 2012; Burggren and Dubansky, 2018). Cutaneous iono/osmoregulatory processes become insufficient before processes associated with respiration, and this is because cutaneous iono/osmoregulatory processes face the same SA/V constraints as respiration, but are further restricted by ion transporters localized within specialized cells known as ionocytes (Li et al., 1995). Functioning ionocytes require an apical membrane that is exposed to the external environment and a basal membrane directly contacting the blood (Alderdice, 1988). As the skin thickens, the likelihood of ionocytes reaching both the external environment and the blood significantly decreases, thus limiting the transport capacity of ionocytes before limitations to respiration occur (Alderdice, 1988). Ionoregulatory mechanisms functioning at the gills prior to respiratory functions have been found in all investigated fishes to date (Rombough, 2002; Fu et al., 2010; Rombough, 1999; Hiroi et al., 1998; Zimmer and Wood, 2015; Zimmer et al., 2014). Iono/osmoregulation, therefore, is increasingly thought to be the primary process underpinning gill development.

The majority of studies investigating the drivers of gill development have focused on model species such as tilapia *Oreochromis mossambicus* (Li et al., 1995), zebrafish, *Danio rerio* (Rombough, 2002), and, most recently, the commercially important rainbow trout, *Oncorhynchus mykiss* (Fu et al., 2010; Zimmer and Wood, 2015; Zimmer et al., 2014). Nevertheless, these species do not represent all fishes, especially fishes living in

[1]ARC Centre of Excellence for Coral Reef Studies, Townsville, QLD 4811, Australia. [2]College of Science and Engineering, James Cook University, Townsville, QLD 4811, Australia. [3]US Geological Survey, Eastern Ecological Science Center, Conte Anadromous Fish Research Laboratory, Turners Falls, MA 01376, USA. [4]Department of Biology, University of Massachusetts, Amherst, MA 01003, USA.

*Author for correspondence (Leteisha.prescott@my.jcu.edu.au)

L.A.P., 0000-0002-3207-2186

Received 17 February 2021; Accepted 25 October 2021

Journal of Experimental Biology (2021) 224, jeb242364. doi:10.1242/jeb.242364

contrasting and challenging ecosystems. Coral reef fishes, during early life stages, often exhibit extreme physiological and demographic characteristics that remain poorly understood. For example, clutch mortality rates during embryogenesis can approach 100% (Emslie and Jones, 2001). During pelagic larval stages, mortality remains extremely high (Goatley and Bellwood, 2016); yet, coral reef fishes have the fastest sustained swimming speeds and highest O_2 uptake rates ($\dot{M}_{O_2}$) relative to their body size of all ectothermic vertebrates studied to date (Nilsson et al., 2007; Stobutzki and Bellwood, 1994, 1997; Fisher et al., 2005; Downie et al., 2020). Upon settlement, coral reef fishes cope with fluctuating O_2 levels that can fall below 20% air saturation at night (Nilsson and Östlund-Nilsson, 2004), making them some of the most hypoxia-tolerant species studied so far (Nilsson et al., 2007). Additionally, developing and residing in tropical, warm waters of coral reefs means these fishes may already live close to their upper thermal limits (Rummer et al., 2014; Gardiner et al., 2010; Johansen and Jones, 2011; Pörtner et al., 2017), accelerating growth and metabolic turnover, and thus creating greater O_2 and carbon dioxide (CO_2) exchange and waste product removal. These aforementioned physiological and demographic characteristics are not yet fully understood, but are almost certainly supported by highly functioning respiratory and ionoregulatory systems. However, the link between gill development and function to support these life history characteristics in coral reef fishes remains unknown. Therefore, expanding our knowledge of gill development in coral reef fishes presents an important opportunity to understand how key developmental events occur in species with unique physiological traits and a challenging environment shaped by high mortality rates.

Here, we examined embryonic development in two coral reef damselfish species to generate a more comprehensive understanding of oxygen uptake and ionoregulatory processes early in the ontogeny of fishes. The aims of this study were to quantify the rate of gill development in reef fish and define when and in what order respiration and ion regulation transitions to the gills. The spiny chromis (*Acanthochromis polyacanthus*) and the cinnamon anemonefish (*Amphiprion melanopus*) were chosen as the study species because they come from one of the most speciose and ecologically dominant coral reef fish families, Pomacentridae (Cowman, 2014; Ceccarelli et al., 2001). The two species also exhibit opposing life histories; *A. polyacanthus* resides on the reef after hatching close to its parents, receiving additional parental care, whereas *A. melanopus* spends its larval phase in the pelagic environment before finding a suitable coral reef habitat on which to settle as a juvenile. For these reasons and others mentioned above, we hypothesize that coral reef fishes will exhibit a rapid rate of development in terms of oxygen uptake and ionoregulatory processes when compared with previously examined species. We might expect to see differences between the two species as a reflection upon their larval life histories. In both species, we examined the gross morphology and histology of gills during early ontogeny. We used respirometry to determine changes in $\dot{M}_{O_2}$ across development, and we used phenylhydrazine (PHZ) to inhibit haemoglobin (Hb) function and provide insights into the role of the gills in respiration. We expect Hb to begin functioning for oxygen transport soon after it first appears to support the aerobically demanding early life history traits of coral reef fishes (i.e. strong swimming abilities and very high mass-specific $\dot{M}_{O_2}$). PHZ destroys Hb indirectly by oxidizing the haeme group (Fe^{3+}; methaemoglobin), which causes Heinz body formation, and ultimately decreases red blood cell (RBC) concentrations and the blood's capacity for oxygen binding and transport (Shetlar and Hill, 1985). Key components of ionoregulatory functions were explored by documenting the appearance of ionocytes within cutaneous and branchial locations using immunocytochemistry. These techniques allowed us to estimate when gills begin functioning for oxygen uptake and ion regulation, and to produce a time line of these traits to compare with other, previously described species.

MATERIALS AND METHODS

James Cook University Animal Ethics Committee approved the following experiments under ethics protocol A2407. Import of antibodies into Australia was approved by the Australian Government, Department of Agriculture and Water Resources under permit #0002256071.

Study species and husbandry

Embryos from *Acanthochromis polyacanthus* (Bleeker 1855) and *Amphiprion melanopus* Bleeker 1852 were sourced from established breeding pairs held in 60 l holding tanks (~4000 l recirculating system; UV-filtered seawater) in aquaria facilities at the Marine and Aquaculture Research Facility at James Cook University. Breeding pairs were exposed to ambient summer photoperiod (approximately 14 h:10 h light:dark), salinity was maintained at 36 ppt, water temperature at 28.5±1°C, and fish were provided with half a terracotta pot for shelter and embryo deposition. Fish were fed twice daily (morning and evening) to satiation with INVE Aquaculture NRD 1.2 mm food pellets (ProAqua Pty Ltd, Coorparoo, QLD, Australia). Pots were checked for egg deposition during morning feeding. For experiments, embryos were collected the morning of the trial, which ensured embryos received maximum parental care by remaining with parents until needed. This ranged from 1 day post-deposition until 1 day prior to hatching. For *A. melanopus*, hatching generally occurred at 7 days post-fertilization (dpf), and for *A. polyacanthus*, hatching occurred at 10 dpf. Six embryos per age across a minimum of three breeding pairs were used for histological and immunocytochemistry protocols (Li et al., 1995). For respirometry trials, a minimum of 10 embryos (Pasparakis et al., 2016) obtained from at least three breeding pairs were used per age and treatment.

Histological techniques: sampling and assays

Embryos were removed from pots and examined under a dissecting microscope (Olympus SZX7 Stereomicroscope System) to observe the onset of the heartbeat, red blood and the presence of gills. Micrographs of the embryos were obtained using an Olympus SC50 digital camera. Embryos were then euthanized by being placed into ice cold water and fixed in Bouin's solution, where they remained for 12–24 h before being transferred into 70% ethanol, where they remained until histological preparation.

To prepare samples for histological assays, all embryos were dechorionated under a dissecting microscope (Olympus SZX7 Stereomicroscope System), micrographs were obtained for measurement of total length (measured in ImageJ v.1.51s, National Institutes of Health, Rockville, MD, USA), and embryos were placed into cassettes. Samples underwent a series of ethanol and wax infiltrations (Shandon Southern Duplex Processor BS5), embedded in paraffin blocks (Shandon Histocentre 3, Thermo Electron Corporation), and then sectioned at 5 µm thickness using a microtome. Samples were embedded laterally and sectioned from when gill tissues were first observed (preliminary inspection using a compound microscope, Olympus BX41 Microscope) and then

Journal of Experimental Biology (2021) 224, jeb242364. doi:10.1242/jeb.242364

subsequently sampled every 10–20 µm. In early ages when gill tissue was not yet formed, sections were sampled when adjacent tissues (e.g. eye, trunk and yolk sac) were in view. Slides were stained using Mayer's Hematoxylin and Eosin, and examined under a compound microscope; images were then taken using an Olympus SC50 digital camera. The presence of morphological features including gill arches, rows of filaments and lamellae was recorded from micrographs.

Respirometry experiments: exposure, setup and trials

We measured oxygen uptake rates (reported as $\dot{M}_{O_2}$) in developing embryos (*A. polyacanthus*: 4.9 mg; *A. melanopus*: 1.6 mg) to determine when blood oxygen transport becomes critical across embryogenesis. However, prior to measuring $\dot{M}_{O_2}$, individuals were either control or PHZ exposed (2 mg l^{-1}) for 3 h (Jacob et al., 2002; Pelster and Burggren, 1996). Exposure time and the movement of PHZ across the chorion were determined by examining control and PHZ-exposed embryos under a dissecting microscope (Olympus SZX7 Stereomicroscope System) and characterizing the pigmentation of the blood flow (i.e. after 3 h exposure to PHZ, blood flow appeared clear to yellow in coloration instead of red, indicating that Hb was destroyed; see Fig. S1; Pelster and Burggren, 1996). $\dot{M}_{O_2}$ was subsequently measured in embryos daily, from 1 dpf until hatching. Measurements ceased in all animals upon hatching because mortality was 100% if newly hatched larvae were exposed to PHZ.

The $\dot{M}_{O_2}$ protocol commenced each morning when embryos were removed from their terracotta pots, transferred into one of two exposure tanks and suspended in mesh (1.5 mm×1.5 mm). A continuous stream of air was directed across the mesh-enclosed embryos, where they remained for 3 h either in control (i.e. sham-treated) or PHZ-treated seawater. Tanks were bleached between trials, and PHZ was disposed of according to the Townsville City Council Wastewater Management Policy. Then, embryos were individually placed into plastic wells (6.86 mm diameter), with each well containing 150 µl seawater and sealed with a rubber stopper, and well plates were submerged in a temperature-controlled flow-through water bath (modified from Pasparakis et al., 2016). Each well had an O_2 sensor spot (REDFLASH dye) connected to a FireSting Optical Oxygen Meter (Pyro Science e. K., Aachen, Germany), and O_2 levels (mg l^{-1}) were measured continuously (every 2 s) over 1 h to determine the embryos' $\dot{M}_{O_2}$. The system was found to be non-permeable by measuring O_2 levels in deoxygenated water for 2 h, a duration which exceeded the experimental period. For analyses, $\dot{M}_{O_2}$ was calculated using the following equation:

$$\dot{M}_{O_2} = SV_{resp}M^{-1}, \quad (1)$$

where S is the slope (mg O_2 l^{-1} h^{-1}), V_{resp} is the volume (l) of the well minus the volume of the embryo, and M is the mass of the embryo (kg) (Rummer et al., 2016). Embryos were patted dry to remove residual water and immediately weighed after each respirometry trial (refer to Table S1 for embryo mass). $\dot{M}_{O_2}$ estimates were measured for 10 min, after a 1 min wait period to avoid signal disturbance from the initial transfer. $\dot{M}_{O_2}$ estimates are representative of a stressed state, as no habituation period occurred (Pasparakis et al., 2016), and are more likely to show differences between control and PHZ-exposed embryos if they truly exist.

Immunocytochemistry: preparation, staining and visualization

Embryos were euthanized as described above and fixed in 4% paraformaldehyde for 24 h at room temperature before being transferred into 70% ethanol and stored at 2°C until further analysis. To prepare embryos for immunocytochemistry, embryos were dechorionated using super fine tip forceps (Dumont) under a dissecting microscope (Olympus SZX7 Stereomicroscope System) and photographed using an Olympus SC50 digital camera for total length. All immunocytochemistry protocols were obtained and modified from McCormick et al. (2003) and Hiroi et al. (2008). Wholemount preparation was used to observe the skin and yolk sac, whereas, sectional preparation was used to observe gill tissue.

Wholemount preparation

Dechorionated embryos were rinsed in 0.01 mol l^{-1} phosphate-buffered saline (PBS; 0.138 mol l^{-1} NaCl, 1.9 mmol l^{-1} NaH_2PO_4, 8.1 mmol l^{-1} Na_2HPO_4 in deionized water, pH 7.4) for 15 min at room temperature, rinsed again in 30% sucrose/PBS solution, and rinsed a third time in PBS before a 30 min incubation in 2% normal goat serum.

Sectional preparation

Similar to wholemount preparation, dechorionated embryos were rinsed in 0.01 mol l^{-1} PBS for 15 min at room temperature and then rinsed again in 30% sucrose/PBS solution before being placed into Cryomolds, covered with embedding medium and frozen at −20°C.

Sections were cut to 5 µm (−20°C; samples were positioned and sectioned as described above) using a Leica CM1860 UV Cryostat and placed on slides to dry. Slides were rinsed with PBS following a 30 min incubation in 2% normal goat serum. Slides and wholemounts were incubated in α5 anti-Na^+,K^+-ATPase antibody (monoclonal; α5 was designed to a highly conserved region of Na^+, K^+-ATPase and deposited in the Developmental Studies Hybridoma Bank by D. M. Fambrough) at 1:1500 dilution in antibody dilution buffer (0.01% NaN_3, 0.1% bovine serum albumin, 2% normal goat serum and 0.02% keyhole limpet hemocyanin in PBS) overnight at 4°C to label ionocytes. The following morning, the samples were rinsed with PBS and incubated a final time with 1:1000 Alexa 488 goat anti-mouse (Life Technologies Australia Pty Ltd, Mulgrave, VIC, Australia) for 2 h at room temperature and rinsed with PBS.

Wholemounts and sectioned samples were examined on an inverted confocal fluorescence microscope (Zeiss LSM 710). Images were taken using Zen 2009 Light Edition (v.5.5.285) confocal software, using a combination of *z*-stacks and continuous imaging. To analyse images obtained from wholemount samples, ionocyte density and size were measured in ImageJ (v.1.51s, National Institutes of Health) and recorded in regard to their location. A grading system (as described by Hiroi et al., 1998) was used for sectional samples of gills obtained because of the complex structure and size of the developing gill tissue. Grades were given to each sample as follows after visually inspecting four individual sections (see Fig. 4 for visible progression of ionocyte density; Hiroi et al., 1998): 0, absent (no ionocytes visible); 1, sparse (some ionocytes visible); 2, moderately dense (several clusters of ionocytes but some areas on filament without ionocytes); or 3, highly dense (filament tissue completely covered with ionocytes or majority covered with minimal areas lacking ionocytes).

Statistical analyses

All statistical analyses were performed in R version 1.1.453. Linear mixed-effects models (LME; nlme package) were used to observe

Journal of Experimental Biology (2021) 224, jeb242364. doi:10.1242/jeb.242364

changes in $\dot{M}_{O_2}$ as a function of embryonic age (dpf). Model selection was conducted by removing non-significant main effects or interactions, except for mass, which was always included in the model. Once visually assessed through Q–Q plots and residual versus fitted plots and compared against un-transformed $\dot{M}_{O_2}$ data using the Akaike information criterion (AIC), $\dot{M}_{O_2}$ was log transformed for both species to meet assumptions of normality. In LMEs for both species, logged $\dot{M}_{O_2}$ was used as a response variable, age and treatment were fixed effects, mass was used as a covariate and clutch was used as a random effect.

LME models were also used to determine changes in ionocyte density and size as a function of embryonic age (dpf). Model selection was conducted by removing non-significant main effects or interactions. Models were visually assessed through Q–Q plots and residuals versus fitted plots to assess normality and equal variances. As a result, and upon comparison with un-transformed $\dot{M}_{O_2}$ data using AIC, ionocyte size was log transformed for both species to meet normality. In the LMEs for both species, ionocyte density or logged size was used as the response variable with age and tissue as fixed effects, and clutch was included as a random effect.

LME models with significant interactions and main effects (i.e. if no significant interaction was detected) were compared using estimated marginal means (EMMs; emmeans package) by comparing the specified variable(s) in the model.

RESULTS

Developmental sequence

In *A. polyacanthus*, at 1 dpf, the yolk sac and rudimentary body and head regions were evident. At 2 and 3 dpf, the heart began to beat, and red blood cells started circulating (Fig. 1). Gill arches appeared as early as 3 dpf but were evident by 4 dpf in all investigated embryos (Fig. 1). After gill arches formed, gill filaments were evident, appearing between 4 and 5 dpf, but most commonly at 5 dpf (Figs 1 and 2), after which, lamellar formation occurred. Lamellae were visualized as early as 5 dpf, most commonly appearing at 6–7 dpf (Figs 1 and 2), but as late as 8 dpf. At 8 and 9 dpf, lamellae proliferated across all filaments. Hatching generally occurred at 10 dpf (±1 dpf).

In *Amphiprion melanopus*, the yolk sac and rudimentary body and head regions were evident at 1 dpf. The heart began to beat and red blood cells started circulating at 2 and 3 dpf, respectively (Fig. 1). In the majority of *A. melanopus* embryos examined, gill arches formed at 3 dpf (Fig. 2); however, in one embryo, gill arches formed at 4 dpf (Fig. 1). Gill filaments appeared predominantly at 4 dpf, but in all embryos by 5 dpf. Lamellae formed soon after at 5 dpf (Fig. 1), although one *A. melanopus* embryo was found to develop lamellae at 6 dpf (Fig. 1). Hatching occurred at 7 dpf (±1 dpf).

Oxygen uptake rate

Significant differences in $\dot{M}_{O_2}$ were detected in *A. polyacanthus* between treatments (LME, $F_{1,370}$=4.7331, P=0.0302) and among ages (LME, $F_{8,370}$=3.2493, P=0.0014; Table S2), whereas treatment (LME, $F_{1,262}$=0.002, P=0.9671) and age (LME, $F_{5,262}$=0.161, P=0.9766) were not significant in *A. melanopus*. In *A. polyacanthus*, PHZ-exposed embryos exhibited an $\dot{M}_{O_2}$ that was 4% (0.174±0.0705 mg O_2 kg^{-1} h^{-1} log transformed; t_{370}=2.468, P=0.0140) lower than in control embryos. In both species, $\dot{M}_{O_2}$ increased with age, as expected (Fig. 3), although this trend was not significant in *A. melanopus*. In *A. polyacanthus*, age was only significant between 1 and 3 dpf, as well as between 3 and 7 dpf (P<0.05; Table S2). Significant interactions between $\dot{M}_{O_2}$ and age and treatment were not detected in either species (P>0.05; removed from model); however, 100% mortality occurred in all fish exposed to PHZ at hatching.

Appearance of ionocytes

Extra-branchial ionocytes first appeared in the yolk sac and trunk (i.e. the skin covering the main body compartment) at 2 dpf in *A. polyacanthus* but at 1 dpf in *A. melanopus* (Fig. 4). In *A. polyacanthus*, a significant interaction was detected between ionocyte density and age and location (LME, $F_{7,89}$=3.5765, P=0.002; Table S3). Ionocyte density increased significantly in

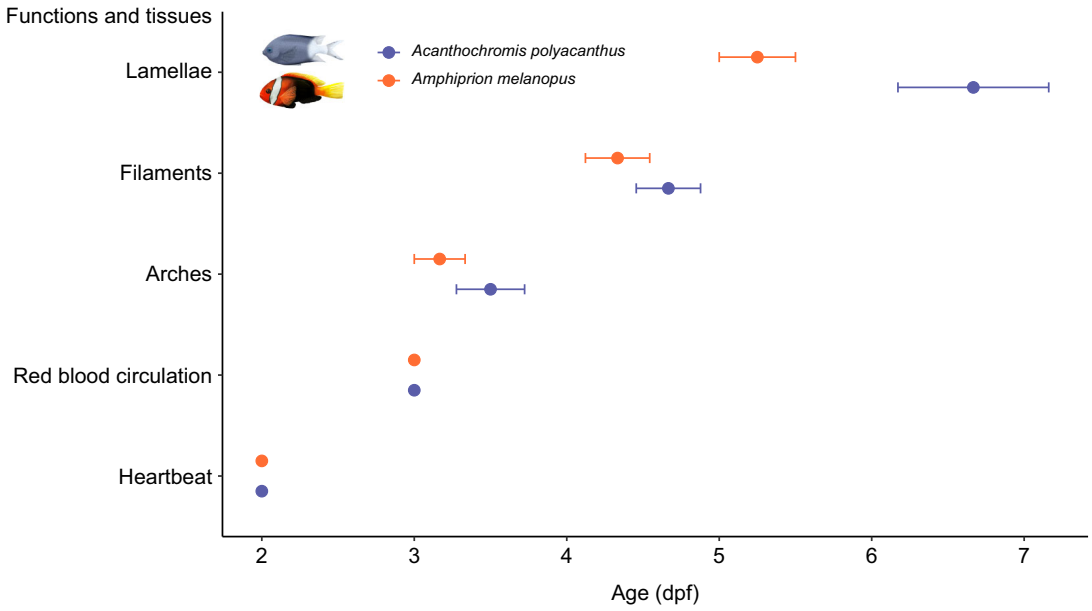

Fig. 1. Sequential appearance of functions and tissues in developing *Acanthochromis polyacanthus* and *Amphiprion melanopus* embryos. All data are means±s.e.m.; n=6 per age. dpf, days post-fertilization.

Journal of Experimental Biology

Journal of Experimental Biology (2021) 224, jeb242364. doi:10.1242/jeb.242364

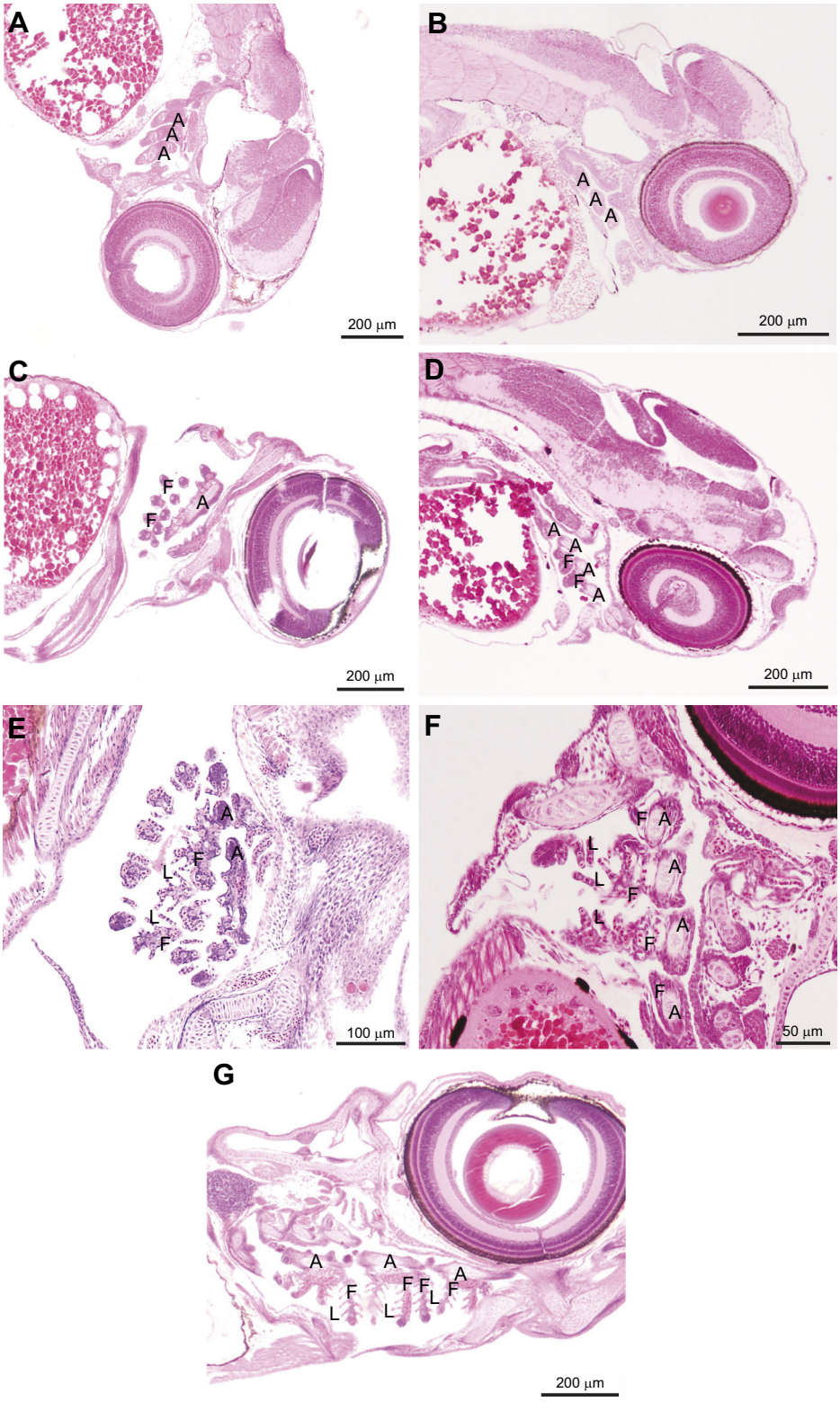

Fig. 2. Histological micrographs of gill development in *A. polyacanthus* and *A. melanopus* embryos. *Acanthochromis polyacanthus* at (A) 4 dpf, (C) 5 dpf, (E) 7 dpf and (G) 9 dpf. *Amphiprion melanopus* at (B) 3 dpf, (D) 5 dpf and (F) 6 dpf. Micrographs were stained with Haematoxylin and Eosin. A, arches; F, filament; L, lamellae. *n*=6 per age.

the trunk of *A. polyacanthus* embryos at 4–5 dpf (an increase of 500%; Fig. 5A; Table S4), after which (i.e. 6–9 dpf), ionocyte density decreased back to similar levels to those estimated at 2–3 dpf (Fig. 5A; Table S4). Ionocyte density in the yolk sac remained similar across development (Figs 4A and 5A; Table S3). In *A. melanopus*, no significant changes in ionocyte density in either tissue were found over increasing embryonic age (Fig. 5B; Table S3). However, ionocyte size changed significantly in both locations (LME, $F_{5,810}$=2.525, P=0.028; Table S3), decreasing by 60% and 67% in the trunk and yolk sac of *A. melanopus* with increasing age (LME, $P \leq 0.05$; Fig. 6B; Table S5). Similarly, in *A. polyacanthus*, ionocyte size in the yolk sac decreased with increasing age (~60% decrease; LME, $P \leq 0.05$), although ionocytes at 9 dpf were not significantly different in size from

Journal of Experimental Biology (2021) 224, jeb242364. doi:10.1242/jeb.242364

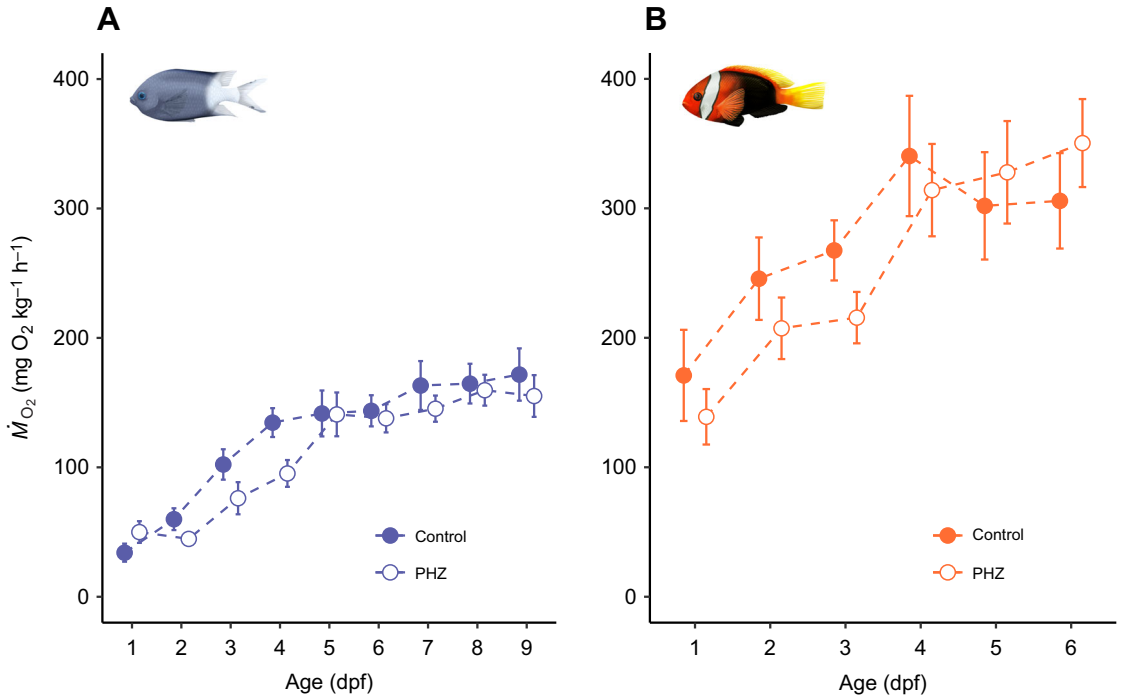

Fig. 3. Oxygen uptake rate ($\dot{M}_{O_2}$) throughout embryonic development following phenylhydrazine (PHZ) treatment. (A) *Acanthochromis polyacanthus* and (B) *A. melanopus*. All data are means±s.e.m. In both species, after hatching, exposure to PHZ resulted in 100% mortality ($n \geq 10$ per age and treatment).

those at 5 and 6 dpf (Fig. 6A; Table S5). Along the trunk of *A. polyacanthus*, ionocyte size changed with age (LME, $P \leq 0.05$); however, the trend was not the same as it was in other tissues (Fig. 6A; Table S5).

In both species, branchial ionocytes were only found in the gill filaments, at the base of the lamellae (interlamellar region), although not in the lamellae themselves (Fig. 4). Ionocytes appeared as soon as filaments started to form, which occurred at 4–5 dpf in *A. polyacanthus* and at 4 dpf in *A. melanopus* (Fig. 7). Moderately to highly dense clusters of ionocytes were found in the filaments at 7 dpf in *A. polyacanthus*, and moderately dense clusters were found at 5 dpf in *A. melanopus*, simultaneous with the formation of lamellae (Fig. 7).

DISCUSSION

Our results show that, when compared with most of the previously investigated fishes, *A. polyacanthus* and *A. melanopus* exhibit rapid gill development during embryogenesis. It is likely that, during embryonic development, the gills have limited contributions to the overall respiratory and ionoregulatory functions, but rather are preparing to become the primary site for these functions upon hatching. This pattern of early gill formation may occur to sustain the high demands of the challenging lifestyle that coral reef fishes endure post-hatching and when the larvae transition from the pelagic environment to metamorphose into juveniles that reside on tropical coral reefs. Coral reef fishes have inherently high mortality rates (Emslie and Jones, 2001; Goatley and Bellwood, 2016), and this may be related to mismatches between the fast pace of development and the efficiency of key physiological functions. Disruptions to gill development during embryogenesis and to gill functions during the larval phases may become more frequent and intense with increasing anthropogenic stressors, perhaps exacerbating the already high mortality rates of this group of coral reef fishes.

In this study, filament and lamellar formation were evident by 5 and 7 dpf, respectively, in *A. melanopus* and *A. polyacanthus*. At 1 day prior to hatching, gill structure in both species started resembling those of juvenile and adult fishes, although they were smaller in size (i.e. transitioning from bud-like structures to a more defined elongated shape; Rombough, 2011). In the majority of fish species that have been investigated to date, gill development does not commence until late in embryonic development, with respiratory tissues, including lamellae, often forming after hatching (Li et al., 1995; Gao et al., 2016; Padrós et al., 2011; Hachero-Cruzado et al., 2009; Rombough, 2002; Rombough, 1999; Hwang, 1990). This is probably due to other environmental parameters influencing their developmental pace (Burggren and Dubansky, 2018). The freshwater cichlids (e.g. tilapia) were previously thought to exhibit the fastest rate of gill development among fishes, with the first signs of gills noted at 7 dpf or 2 days post-hatching (dph; Li et al., 1995); however, more recently studies have shown that zebrafish (*Danio rerio*) begin gill development at 3 dpf with lamellae forming later at 12 dpf (Rombough, 2002), and the tropical gar (*Atractosteus tropicus*) form gill filaments at 5.5–6.5 dpf or 2.5 dph, with lamellae formation beginning at 11–12 dpf or 9 dph (Burggren et al., 2016). The species examined in the present study, therefore, fall within the high extremes of known developmental rates among teleost fishes.

Alongside rapid structural development, oxygen demand (measured as $\dot{M}_{O_2}$ in this study) also increases during embryogenesis, peaking between 5 and 7 dpf. During embryogenesis, oxygen uptake rates in these two damselfish species were unaffected by PHZ exposure regardless of age; however, PHZ-treated embryos did exhibit a trend of having a lower $\dot{M}_{O_2}$ than control embryos, but this trend was not significant until hatching. This suggests that Hb – during embryogenesis – does not playing a key role in oxygen uptake, unlike what has been documented in the majority of adult teleost fishes (Cameron and

Journal of Experimental Biology (2021) 224, jeb242364. doi:10.1242/jeb.242364

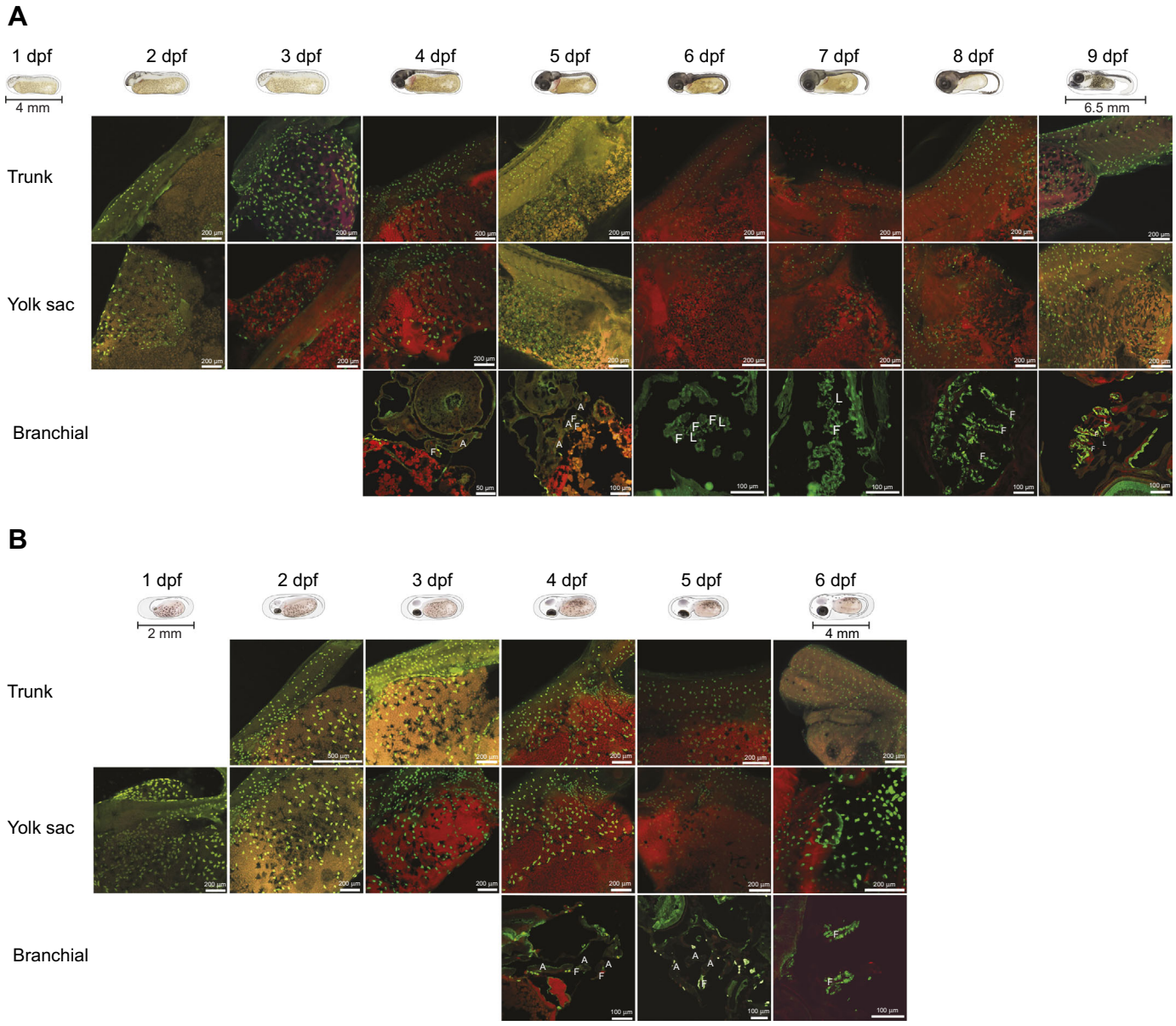

Fig. 4. Appearance of ionocytes along the skin, yolk sac and branchial regions throughout embryonic development. Ionocytes were labelled using anti-Na^+,K^+-ATPase antibody (green). In the branchial micrographs of *A. polyacanthus* (A), 4 and 5 dpf represent a grade between (0) absent and (1) sparse, where ionocytes are visible in some filaments but not all; 6 dpf was graded as (1) sparse; 7 dpf was graded as (2) moderately dense; and 8–9 dpf was graded as (3) highly dense, where filament tissue appears to be completely covered in ionocytes. In the branchial micrographs of *A. melanopus* (B), 4 dpf was graded as (1) sparse; 5 dpf was graded as (2) moderately dense; and 6 dpf was graded as (3) highly dense. A, arches; F, filament; L, lamellae. *n*=6.

Wohlschlag, 1969). Indeed, during embryogenesis, oxygen uptake in these two damselfish species is most likely occurring across the skin epithelium (Feder and Burggren, 1985; Pelster and Burggren, 1996), but they become reliant on Hb for O_2 transport during their larval stage, possibly related to the onset of their profound swimming abilities and increased mass-specific $\dot{M}_{O_2}$. This finding shows that these two study species develop Hb O_2 transport rapidly and early in ontogeny. This change in Hb O_2 transport before and after hatching is surprising, given that $\dot{M}_{O_2}$ in zebrafish at hatching (<4 dpf) was unaffected by PHZ treatment at similar exposure levels (Pelster and Burggren, 1996), but showed similar trends (i.e. lower $\dot{M}_{O_2}$ with PHZ exposure). Although $\dot{M}_{O_2}$ in PHZ-exposed embryos was not significantly lower than that in control embryos, Hb may still be playing some role in O_2 transport that was not captured in this experiment; for example, because of a lack of sufficient water flow across the gills due to irregular buccal pumping during early development (Rombough, 2011). Moreover, fine scale measurements (e.g. hourly) may provide greater insight. Future investigations should focus on early development of oxygen uptake machinery, the transition from cutaneous to branchial pathways, and Hb O_2 transport activation in coral reef fish embryos and early life stages of other fish species.

We also found early development of key components of the ionoregulatory system in both *A. polyacanthus* and *A. melanopus* when compared with previously studied teleosts. Ionocytes first appeared on the gills at 3 dpf, simultaneously with gill arch and filament formation, thus outpacing zebrafish (5.5 dpf; Rombough, 2002). Moreover, ionocyte density increased substantially during this short developmental window between 4 and 6 dpf, a period coinciding with a decreased density of cutaneous ionocytes

Journal of Experimental Biology (2021) 224, jeb242364. doi:10.1242/jeb.242364

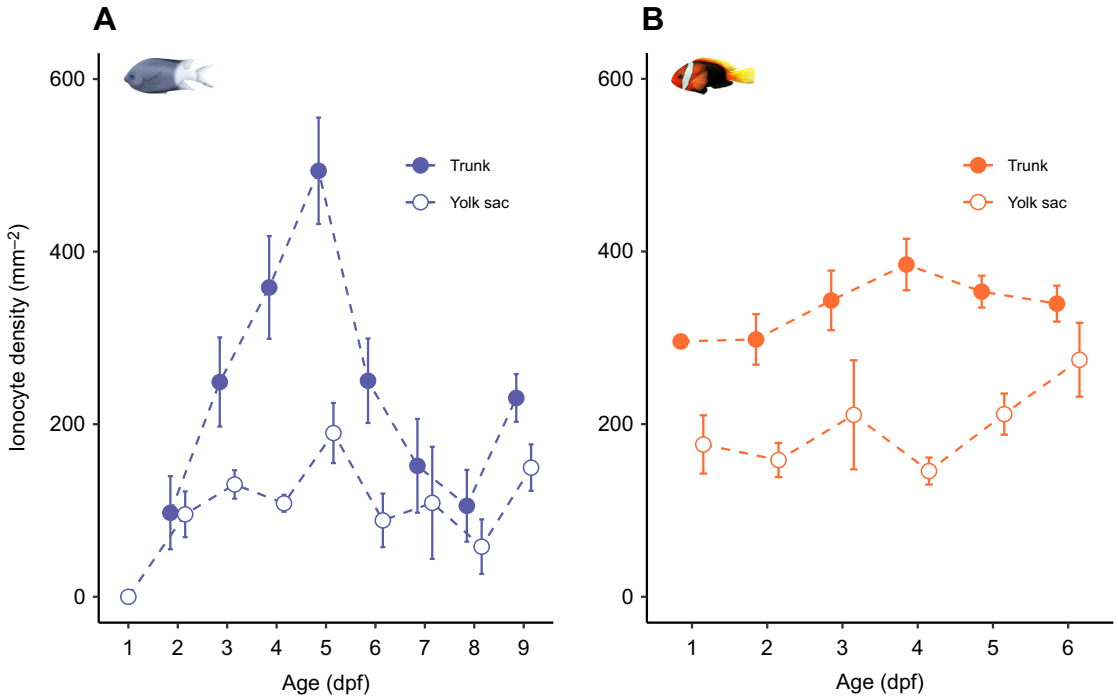

Fig. 5. Changes in ionocyte density across age in the trunk and yolk sac. (A) *Acanthochromis polyacanthus* and (B) *A. melanopus*. All data are means±s.e.m.; *n*=6 per age.

in *A. polyacanthus* and a decrease in cutaneous ionocyte size in both species. Morphometric changes to cutaneous ionocytes that coincide with rapid expansion of branchial ionocytes may indicate the onset of ionoregulatory processes transitioning to the gills.

This accelerated pace of gill development observed in these two coral reef fish species may occur for a number of reasons. Marine fishes are faced with greater ionoregulatory and oxygen uptake limitations than freshwater fishes because oxygen solubility is lower in seawater than in freshwater. The energetic requirements of osmoregulation are thought to be higher in seawater than in freshwater, though the precise requirements for each are still unknown (Kirschner, 1995; Ern et al., 2014). Additionally, ectothermic, tropical species exhibit higher metabolic rates than their temperate water counterparts (Angilletta et al., 2002; Pörtner et al., 2017), therefore creating immense pressure on physiological systems to ensure efficient gas exchange and ion balance. Rapid onset of gill development may also be a necessary response to high mortality rates endured by these coral reef fish species and the overall challenging lifestyle of coral reefs (Goatley and Bellwood, 2016; Emslie and Jones, 2001). Therefore, the rapid gill development documented for these two species of coral reef fishes may be related to the fact that they are marine, tropical ectotherms, and coral reef fish species, or a combination thereof.

Larval coral reef fishes exhibit an array of early life history traits that are likely to rely on the rapid pace of gill development observed in this study. Firstly, coral reef fishes exhibit high growth rates (e.g. organogenesis and morphogenesis) and rapid yolk sac consumption (Green and McCormick, 2001; Donelson et al., 2012), generating high loads of metabolic waste (Wright et al., 1995; Dhiyebi et al., 2013; Zimmer et al., 2014). During early life stages, nitrogenous waste must be removed through Na^+/NH_4^+ exchangers that are located within cutaneous ionocytes; such cutaneous processes are curtailed with declining SA/V ratios of embryos, thus necessitating increasing reliance on branchial pathways. Secondly, larval coral reef fishes undergo major changes in aerobic capacity upon hatching, which may be related to early gill development, both structurally and physiologically. Of all coral reef fishes, the pomacentrids have been investigated most thoroughly with respect to metabolic performance and exhibit among the highest recorded mass-specific $\dot{M}_{O_2}$ (e.g. 5250 mg kg^{-1} h^{-1}) for ectothermic vertebrates (Nilsson et al., 2007) and the fastest sustained swimming speeds (i.e. approximately 50 body lengths per second) examined to date (Stobutzki and Bellwood, 1994, 1997; Downie et al., 2020). Our results suggest that these high demands may be aided by structural and functional changes to the gills during early development, including enhanced structure for ion transport and increased aerobic capacity.

Understanding whether gills form primarily for respiratory or ionoregulatory purposes is crucial to identifying the processes driving the evolution and development of fishes. For example, Fu et al. (2010) and Zimmer et al. (2014) found that Na^+ and NH_4^+ movements in rainbow trout larvae transitioned from cutaneous pathways to the gills simultaneously at 15 dph, but before O_2 uptake, which occurred at 27 dph (Zimmer et al., 2014). These authors also provide evidence supporting sodium uptake and ammonia excretion as one of the first functions performed by the developing gill, thus supporting the ionoregulatory hypothesis. Our study did not directly distinguish between cutaneous and branchial pathways for respiration and ionoregulation. However, our study shows that ionoregulatory tissues (i.e. gill filaments) and ionocytes appear prior to respiratory tissue (i.e. gill lamellae) formation and before respiration becomes dependent on the gills, suggesting that gills may initially function for ionoregulatory processes in these coral reef fish species as well. The presence of ionocytes in gill filaments prior to lamellae formation is a phenomenon that has been observed in numerous fish species (Li et al., 1995; Gao et al., 2016;

Journal of Experimental Biology (2021) 224, jeb242364. doi:10.1242/jeb.242364

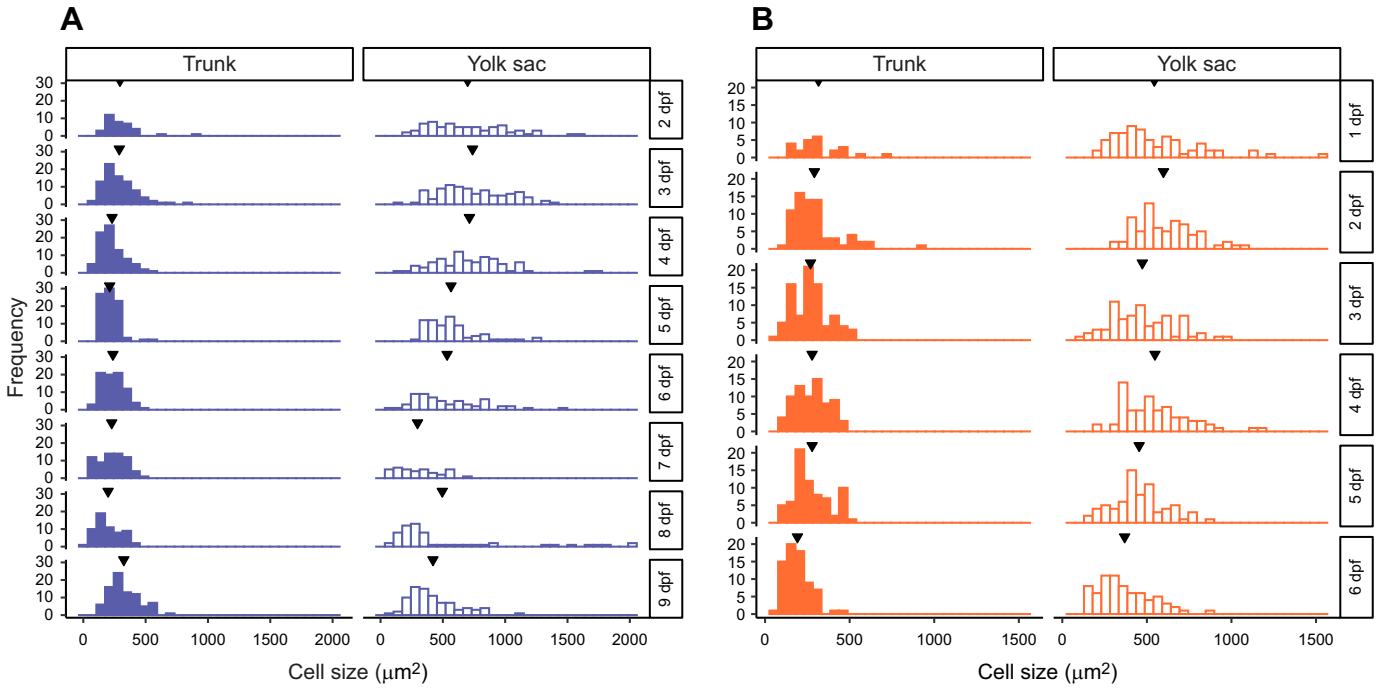

Fig. 6. Frequency histogram showing changes in ionocyte size with age in the trunk and yolk sac. (A) *Acanthochromis polyacanthus* and (B) *A. melanopus*. Arrowheads indicate mean cell size of ionocytes at each location. *n*=6.

Padrós et al., 2011; Hachero-Cruzado et al., 2009; Rombough, 2002, 1999; Hwang, 1990), suggesting that gills perform ionoregulatory processes first. Therefore, our findings also lend support to the ionoregulatory hypothesis. Although morphological trends of ionocytes can be used as a tool to determine the onset of ionoregulatory processes at the gills (Brauner and Rombough, 2012), this only approximates the relative roles of cutaneous and branchial mechanisms at this stage of development.

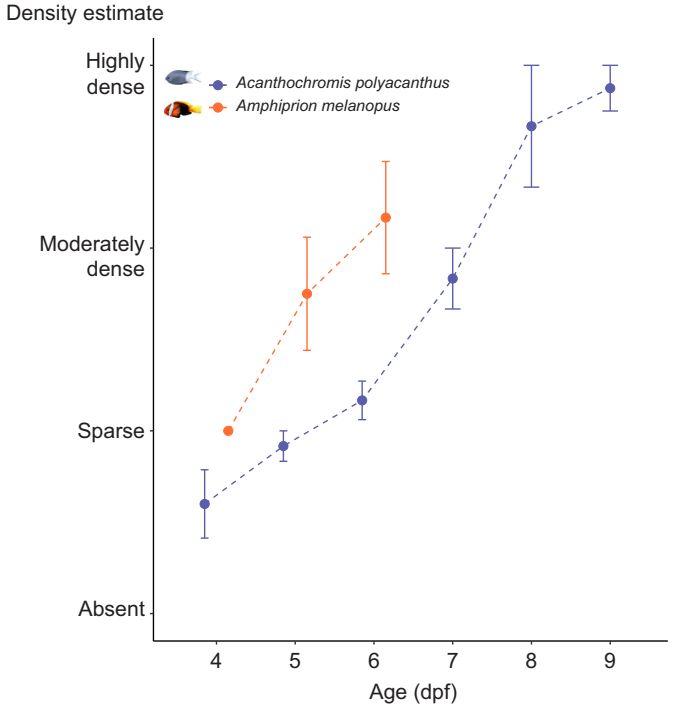

Fig. 7. Changes in ionocyte density with age in gill filaments of *A. polyacanthus* and *A. melanopus*. All data are means±s.e.m.; *n*=6.

Further investigation is needed to determine when and in what order the respiratory and ionoregulatory processes transition from the cutaneous surfaces to the gills in coral reef fishes (i.e. oxygen versus ionoregulatory hypothesis). Coral reef fishes present a unique group that contrast with previously investigated teleost fishes, as they exhibit physiologically demanding life history traits that are most likely the definitive drivers underpinning early gill development. With this information, we can then identify potential mismatches between gill development and function and whether this is related to high mortality rates exhibited during their larval phase. This information should be extremely powerful in determining how anthropogenic stressors interfere with growth and survival, especially during key developmental windows, which could collectively improve predictions for future coral reef fish populations.

In summary, gill formation during embryonic development in coral reef fishes occurs at a rapid rate, perhaps to support high-performance traits exhibited during their larval life stage and in preparation for the challenging lifestyle on tropical coral reefs. Many coral reef fish species have now been documented to possess high $\dot{M}_{O_2}$, fast swimming speeds and remarkable hypoxia tolerance (Leis and McCormick, 2002; Stobutzki and Bellwood, 1994, 1997; Nilsson et al., 2007); therefore, it is likely that the fast-paced developmental patterns observed here may extend beyond these two study species and beyond species within the Family Pomacentridae. Furthermore, this study has outlined a critical developmental window in two coral reef fish species, perhaps one that may be common for other coral reef fish species. This developmental window may therefore be an appropriate target for future investigations, in particular when identifying potential mismatches between environmental pressures and the pace at which these key respiratory and ionoregulatory systems develop.

Acknowledgements
The authors thank the J.L.R. and S.D.M. labs for their assistance with animal husbandry, Adam Downie and Bjorn Illing for all their insight and helpful discussions, James Cook University Marine and Aquaculture Facilities for resources, M. J. McWilliam for editorial work, R. Jones for statistical advice, S. and L. Reilly, K. Cuthbertson and S. Askew for immunocytochemical and histological support, and E. Walsh for illustrations. Any use of trade, product, or firm names in this paper is for descriptive purposes only and does not imply endorsement by the US Government.

Competing interests
The authors declare no competing or financial interests.

Author contributions
Conceptualization: J.L.R.; Methodology: L.A.P., A.M.R., S.J.M., S.D.M., J.L.R.; Formal analysis: L.A.P.; Investigation: L.A.P.; Resources: A.M.R., S.J.M., S.D.M., J.L.R.; Writing - original draft: L.A.P.; Writing - review & editing: L.A.P., A.M.R., S.J.M., S.D.M., J.L.R.; Supervision: J.L.R.; Project administration: J.L.R.; Funding acquisition: J.L.R.

Funding
This project was supported by an Australian Research Council (ARC) Early Career Discovery Fellowship (PDE150101266) and a research allocation from the ARC Centre of Excellence for Coral Reef Studies to J.L.R.

Data availability
The supporting datafile can be accessed through James Cook University's research data repository (Tropical Data Hub): https://research.jcu.edu.au/researchdata/default/detail/70d8a65388c8e5960c559f1aa4c45781/

References

Alderdice, D. F. (1988). Osmotic and ionic regulation in teleost eggs and larvae. *Fish Physiol.* **11**, 163-251. doi:10.1016/S1546-5098(08)60200-9
Angilletta, M. J., , Jr., Niewiarowski, P. H. and Navas, C. A. (2002). The evolution of thermal physiology in ectotherms. *J. Therm. Biol.* **27**, 249-268. doi:10.1016/S0306-4565(01)00094-8
Baker, D. W., Sardella, B., Rummer, J. L., Sackville, M. and Brauner, C. J. (2015). Hagfish: champions of CO_2 tolerance question the origins of vertebrate gill function. *Sci. Rep.* **5**, 11182. doi:10.1038/srep11182
Berry, K. L. E., Hoogenboom, M. O., Flores, F. and Negri, A. P. (2016). Simulated coal spill causes mortality and growth inhibition in tropical marine organisms. *Sci. Rep.* **6**, 25894. doi:10.1038/srep25894
Brauner, C. J. and Rombough, P. J. (2012). Ontogeny and paleophysiology of the gill: new insights from larval and air-breathing fish. *Respir. Physiol. Neurobiol.* **184**, 293-300. doi:10.1016/j.resp.2012.07.011
Burggren, W. and Dubansky, B. (2018). *Development and Environment, S.l.*, Springer International Publishing.
Burggren, W. W. and Pinder, A. W. (1991). Ontogeny of cardiovascular and respiratory physiology in lower vertebrates. *Annu. Rev. Physiol.* **53**, 107-135. doi:10.1146/annurev.ph.53.030191.000543
Burggren, W. W., Bautista, G. M., Coop, S. C., Couturier, G. M., Delgadillo, S. P., García, R. M. and González, C. A. A. (2016). Developmental cardiorespiratory physiology of the air-breathing tropical gar, Atractosteus tropicus. *Am. J. Physiol. Regul. Integr. Comp. Physiol.* **311**, R689-R701. doi:10.1152/ajpregu.00022.2016
Cameron, J. N. and Wohlschlag, D. E. (1969). Respiratory response to experimentally induced anaemia in the pinfish (Lagodon rhomboides). *J. Exp. Biol.* **50**, 307-317. doi:10.1242/jeb.50.2.307
Ceccarelli, D. M., Jones, G. P. and McCook, L. J. (2001). Territorial damselfishes as determinants of the structure of benthic communities on coral reefs. In *Oceanography and Marine Biology, An Annual Review*, **Vol. 39** (ed. R. N. Gibson, R. N. Gibson). CRC Press.
Cowman, P. F. (2014). Historical factors that have shaped the evolution of tropical reef fishes: a review of phylogenies, biogeography, and remaining questions. *Front. Genet.* **5**, 394. doi:10.3389/fgene.2014.00394
Dhiyebi, H. A., O'Donnell, M. J. and Wright, P. A. (2013). Water chemistry in the microenvironment of rainbow trout *Oncorhynchus mykiss* embryos is affected by development, the egg capsule and crowding. *J. Fish Biol.* **82**, 444-457.
Donelson, J. M., Munday, P. L. and McCormick, M. I. (2012). Climate change may affect fish through an interaction of parental and juvenile environments. *Coral Reefs* **31**, 753-762. doi:10.1007/s00338-012-0899-7
Downie, A. T., Illing, B., Faria, A. M. and Rummer, J. L. (2020). Swimming performance of marine fish larvae: review of a universal trait under ecological and environmental pressure. *Rev. Fish Biol. Fish.* **30**, 93-108. doi:10.1007/s11160-019-09592-w
Emslie, M. J. and Jones, G. P. (2001). Patterns of embryo mortality in a demersally spawning coral reef fish and the role of predatory fishes. *Environ. Biol. Fishes* **60**, 363-373. doi:10.1023/A:1011069126615
Ern, R., Huong, D. T. T., Cong, N. V., Bayley, M. and Wang, T. (2014). Effect of salinity on oxygen consumption in fishes: a review. *J. Fish Biol.* **84**, 1210-1220. doi:10.1111/jfb.12330
Evans, D. H. (1998). *The Physiology of Fishes*. Boca Raton: CRC Press.
Evans, D. H., Piermarini, P. M. and Choe, K. P. (2005). The multifunctional fish gill: dominant site of gas exchange, osmoregulation, acid-base regulation, and excretion of nitrogenous waste. *Physiol. Rev.* **85**, 97-177. doi:10.1152/physrev.00050.2003
Feder, M. E. and Burggren, W. W. (1985). Cutaneous gas exchange in vertebrates: design, patterns, control and implications. *Biol. Rev.* **60**, 1-45. doi:10.1111/j.1469-185X.1985.tb00416.x
Fisher, R., Leis, J. M., Clark, D. L. and Wilson, S. K. (2005). Critical swimming speeds of late-stage coral reef fish larvae: variation within species, among species and between locations. *Mar. Biol.* **147**, 1201-1212. doi:10.1007/s00227-005-0001-x
Fu, C., Wilson, J. M., Rombough, P. J. and Brauner, C. J. (2010). Ions first: Na^+ uptake shifts from the skin to the gills before O_2 uptake in developing rainbow trout, Oncorhynchus mykiss. *Proc. R. Soc. B Biol. Sci.* **277**, 1553-1560. doi:10.1098/rspb.2009.1545
Gao, X., Hong, L., Liu, Z., Guo, Z., Wang, Y. and Lei, J. (2016). An integrative study of larval organogenesis of American shad Alosa sapidissima in histological aspects. *Chin. J. Oceanol. Limnol.* **34**, 136-152. doi:10.1007/s00343-016-5008-2
Gardiner, N. M., Munday, P. L. and Nilsson, G. E. (2010). Counter-gradient variation in respiratory performance of coral reef fishes at elevated temperatures. *PLoS ONE* **5**, e13299. doi:10.1371/journal.pone.0013299
Goatley, C. H. R. and Bellwood, D. R. (2016). Body size and mortality rates in coral reef fishes: a three-phase relationship. *Proc. R. Soc. B Biol. Sci.* **283**, 20161858. doi:10.1098/rspb.2016.1858
Green, B. S. and McCormick, M. I. (2001). Ontogeny of the digestive and feeding systems in the anemonefish amphiprion melanopus. *Environ. Biol. Fishes* **61**, 73-83. doi:10.1023/A:1011044919990
Hachero-Cruzado, I., Ortiz-Delgado, J. B., Borrega, B., Herrera, M., Navas, J. I. and Sarasquete, C. (2009). Larval organogenesis of flatfish brill Scophthalmus rhombus L: histological and histochemical aspects. *Aquaculture* **286**, 138-149. doi:10.1016/j.aquaculture.2008.09.039
Hess, S., Wenger, A. S., Ainsworth, T. D. and Rummer, J. L. (2015). Exposure of clownfish larvae to suspended sediment levels found on the great barrier reef: impacts on gill structure and microbiome. *Sci. Rep.* **5**, 10561. doi:10.1038/srep10561
Hess, S., Prescott, L. J., Hoey, A. S., McMahon, S. A., Wenger, A. S. and Rummer, J. L. (2017). Species-specific impacts of suspended sediments on gill structure and function in coral reef fishes. *Proc. R. Soc. B Biol. Sci.* **284**, 20171279. doi:10.1098/rspb.2017.1279
Hiroi, J., Kaneko, T., Seikai, T. and Tanaka, M. (1998). Developmental sequence of chloride cells in the body skin and gills of Japanese flounder (Paralichthys olivaceus) larvae. *Zoolog. Sci.* **15**, 455-460. doi:10.2108/0289-0003(1998)15[455:DSOCCI]2.0.CO;2
Hiroi, J., Yasumasu, S., McCormick, S. D., Hwang, P.-P. and Kaneko, T. (2008). Evidence for an apical Na-Cl cotransporter involved in ion uptake in a teleost fish. *J. Exp. Biol.* **211**, 2584-2599. doi:10.1242/jeb.018663
Hwang, P. P. (1990). Salinity effects on development of chloride cells in the larvae of ayu (Plecoglossus altivelis). *Mar. Biol.* **107**, 1-7. doi:10.1007/BF01313236
Jacob, E., Drexel, M., Schwerte, T. and Pelster, B. (2002). Influence of hypoxia and of hypoxemia on the development of cardiac activity in zebrafish larvae. *Am. J. Physiol. Regul. Integr. Comp. Physiol.* **283**, R911-R917. doi:10.1152/ajpregu.00673.2001
Johansen, J. L. and Jones, G. P. (2011). Increasing ocean temperature reduces the metabolic performance and swimming ability of coral reef damselfishes. *Glob. Change Biol.* **17**, 2971-2979. doi:10.1111/j.1365-2486.2011.02436.x
Kimmel, C. B., Ballard, W. W., Kimmel, S. R., Ullmann, B. and Schilling, T. F. (1995). Stages of embryonic development of the zebrafish. *Dev. Dyn.* **203**, 253-310. doi:10.1002/aja.1002030302
Kirschner, L. B. (1995). Energetics of osmoregulation in fresh water vertebrates. *J. Exp. Zool.* **271**, 243-252. doi:10.1002/jez.1402710402
Krogh, A. (1941). *The Comparative Physiology of Respiratory Mechanisms*, New York: Dover Publications.
Leis, J. M. and McCormick, M. I. (2002). The biology, behavior, and ecology of the pelagic, larval stage of coral reef fishes. In *Coral Reef Fishes - Dynamics and Diversity in a Complex Ecosystem* (ed. P. F. Sale), pp. 171-199. Elsevier.
Li, J., Eygensteyn, J., Lock, R., Verbost, P., Heijden, A., Bonga, S. and Flik, G. (1995). Branchial chloride cells in larvae and juveniles of freshwater tilapia Oreochromis mossambicus. *J. Exp. Biol.* **198**, 2177-2184. doi:10.1242/jeb.198.10.2177
McCormick, S. D., Sundell, K., Björnsson, B. T., Brown, C. L. and Hiroi, J. (2003). Influence of salinity on the localization of Na^+/K^+-ATPase,$Na^+/K^+/2Cl^-$ cotransporter (NKCC) and CFTR anion channel in chloride cells of the Hawaiian goby (Stenogobius hawaiiensis). *J. Exp. Biol.* **206**, 4575-4583. doi:10.1242/jeb.00711

Nilsson, G. E. and Östlund-Nilsson, S. (2004). Hypoxia in paradise: widespread hypoxia tolerance in coral reef fishes. *Proc. R. Soc. B Biol. Sci.* **271** Suppl. 3, S30-S33. doi:10.1098/rsbl.2003.0087

Nilsson, G. E., Östlund-Nilsson, S., Penfold, R. and Grutter, A. S. (2007). From record performance to hypoxia tolerance: respiratory transition in damselfish larvae settling on a coral reef. *Proc. R. Soc. B Biol. Sci.* **274**, 79-85. doi:10.1098/rspb.2006.3706

Padrós, F., Villalta, M., Gisbert, E. and Estévez, A. (2011). Morphological and histological study of larval development of the Senegal sole Solea senegalensis: an integrative study. *J. Fish Biol.* **79**, 3-32. doi:10.1111/j.1095-8649.2011.02942.x

Pasparakis, C., Mager, E. M., Stieglitz, J. D., Benetti, D. and Grosell, M. (2016). Effects of Deepwater Horizon crude oil exposure, temperature and developmental stage on oxygen consumption of embryonic and larval mahi-mahi (Coryphaena hippurus). *Aquat. Toxicol.* **181**, 113-123. doi:10.1016/j.aquatox.2016.10.022

Pelster, B. and Burggren, W. W. (1996). Disruption of hemoglobin oxygen transport does not impact oxygen-dependent physiological processes in developing embryos of zebra fish (Danio rerio). *Circ. Res.* **79**, 358-362. doi:10.1161/01.RES.79.2.358

Pörtner, H.-O., Bock, C. and Mark, F. C. (2017). Oxygen- and capacity-limited thermal tolerance: bridging ecology and physiology. *J. Exp. Biol.* **220**, 2685-2696. doi:10.1242/jeb.134585

Rombough, P. J. (1988). 2 respiratory gas exchange, aerobic metabolism, and effects of hypoxia during early life. *Fish Physiol.* **11**, 59-161. doi:10.1016/S1546-5098(08)60199-5

Rombough, P. J. (1998). Partitioning of oxygen uptake between the gills and skin in fish larvae: a novel method for estimating cutaneous oxygen uptake. *J. Exp. Biol.* **201**, 1763-1769. doi:10.1242/jeb.201.11.1763

Rombough, P. J. (1999). The gill of fish larvae. Is it primarily a respiratory or an ionoregulatory structure? *J. Fish Biol.* **55**, 186-204. doi:10.1111/j.1095-8649.1999.tb01055.x

Rombough, P. (2002). Gills are needed for ionoregulation before they are needed for O2 uptake in developing zebrafish, Danio rerio. *J. Exp. Biol.* **205**, 1787-1794. doi:10.1242/jeb.205.12.1787

Rombough, P. (2007). The functional ontogeny of the teleost gill: which comes first, gas or ion exchange? *Comp. Biochem. Physiol. A Mol. Integr. Physiol.* **148**, 732-742. doi:10.1016/j.cbpa.2007.03.007

Rombough, P. J. (2011). Ventilation and animal respiration respiratory gas exchange during development: respiratory transitions. In *Encyclopedia of Fish Physiology* (ed. A. P. Farrell), pp. 838-845. San Diego: Academic Press.

Rombough, P. and Drader, H. (2009). Hemoglobin enhances oxygen uptake in larval zebrafish (Danio rerio) but only under conditions of extreme hypoxia. *J. Exp. Biol.* **212**, 778-784. doi:10.1242/jeb.026575

Rombough, P. and Moroz, B. (1997). The scaling and potential importance of cutaneous and branchial surfaces in respiratory gas exchange in larval and juvenile walleye. *J. Exp. Biol.* **200**, 2459-2468. doi:10.1242/jeb.200.18.2459

Rummer, J. L., Couturier, C. S., Stecyk, J. A. W., Gardiner, N. M., Kinch, J. P., Nilsson, G. E. and Munday, P. L. (2014). Life on the edge: thermal optima for aerobic scope of equatorial reef fishes are close to current day temperatures. *Glob. Change Biol.* **20**, 1055-1066. doi:10.1111/gcb.12455

Rummer, J. L., Binning, S. A., Roche, D. G. and Johansen, J. L. (2016). Methods matter: considering locomotory mode and respirometry technique when estimating metabolic rates of fishes. *Conserv. Physiol.* **4**, cow008. doi:10.1093/conphys/cow008

Shetlar, M. D. and Hill, H. A. (1985). Reactions of hemoglobin with phenylhydrazine: a review of selected aspects. *Environ. Health Perspect.* **64**, 265-281. doi:10.1289/ehp.8564265

Stobutzki, I. C. and Bellwood, D. R. (1994). An analysis of the sustained swimming abilities of pre- and post-settlement coral reef fishes. *J. Exp. Mar. Biol. Ecol.* **175**, 275-286. doi:10.1016/0022-0981(94)90031-0

Stobutzki, I. C. and Bellwood, D. R. (1997). Sustained swimming abilities of the late pelagic stages of coral reef fishes. *Mar. Ecol. Prog. Ser.* **149**, 35-41. doi:10.3354/meps149035

Wright, P., Felskie, A. and Anderson, P. (1995). Induction of ornithine-urea cycle enzymes and nitrogen metabolism and excretion in rainbow trout (*Oncorhynchus mykiss*) during early life stages. *J. Exp. Biol.* **198**, 127-135.

Zimmer, A. M. and Wood, C. M. (2015). Ammonia first? The transition from cutaneous to branchial ammonia excretion in developing rainbow trout is not altered by exposure to chronically high NaCl. *J. Exp. Biol.* **218**, 1467-1470. doi:10.1242/jeb.119362

Zimmer, A. M., Wright, P. A. and Wood, C. M. (2014). What is the primary function of the early teleost gill? Evidence for Na^+/NH_4^+ exchange in developing rainbow trout (Oncorhynchus mykiss). *Proc. R. Soc. B Biol. Sci.* **281**, 20141422. doi:10.1098/rspb.2014.1422

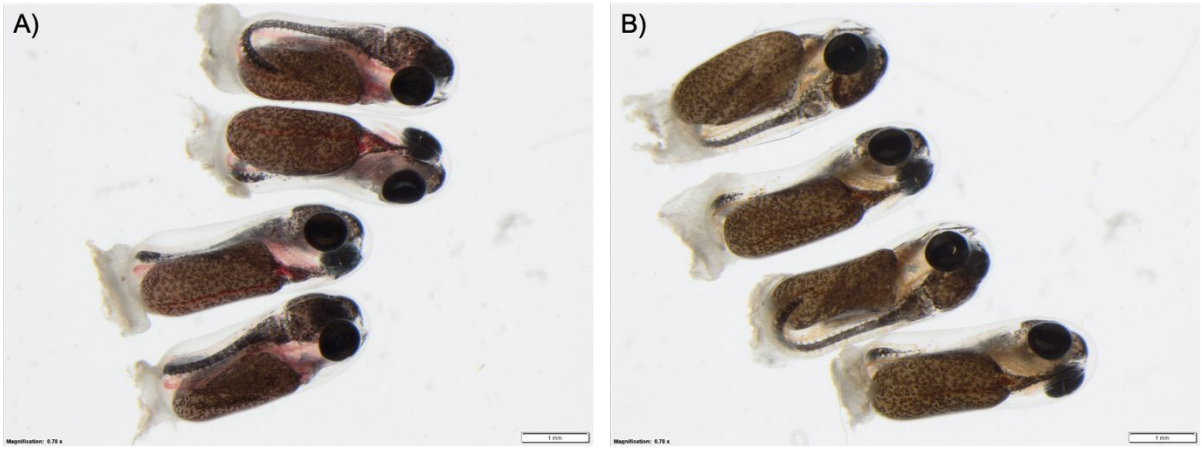

Phenylhydrazine exposure

Fig. S1. Micrographs of *Acanthochromis polyacanthus* embryos at 9 days post fertilization showing: **A)** control embryos with red blood (haemoglobin present) and **B)** phenylhydrazine exposed embryos with yellow-clear blood (haemoglobin destroyed).

Table S1. Mass of *Acanthochromis polyacanthus* and *Amphiprion melanopus* embryos across age (dpf).

Species	Age (dpf)	Mass (kg)	Std. error
Acanthochromis polyacanthus	1	0.004716	0.000139
	2	0.004955	0.000157
	3	0.005028	0.000165
	4	0.004824	0.000139
	5	0.004709	0.000167
	6	0.004911	0.000105
	7	0.004918	0.000121
	8	0.004939	0.000106
	9	0.005166	0.000150
Amphiprion melanopus	1	0.001800	7.06E-05
	2	0.001745	8.43E-05
	3	0.001804	5.52E-05
	4	0.001626	5.79E-05
	5	0.001665	5.24E-05
	6	0.001609	8.15E-05

Table S2. Estimated marginal means statistical output for the comparison of $\dot{M}O_2$ across age in *Acanthochromis polyacanthus* embyos. Results are given on a log scale. Bold text indicates Pr(>|z|) values of significance ($\alpha = 0.05$).

Species	Age (dpf) comparison	Estimate	Std. error	D.F.	t ratio	Pr(>|z|)
Acanthochromis polyacanthus	1-2	-0.43949	0.161142	370	-2.727	0.1419
	1-3	-0.57865	0.163173	370	-3.546	**0.0130**
	1-4	-0.1284	0.158182	370	-0.812	0.9965
	1-5	-0.45743	0.172631	370	-2.650	0.1700
	1-6	-0.33924	0.15436	370	-2.198	0.4093
	1-7	-0.04521	0.164823	370	-0.274	1.0000
	1-8	-0.3306	0.159379	370	-2.074	0.4926
	1-9	-0.20363	0.169269	370	-1.203	0.9556
	2-3	-0.13916	0.150334	370	-0.926	0.9914
	2-4	0.311086	0.143666	370	2.165	0.4307
	2-5	-0.01794	0.158384	370	-0.113	1.0000
	2-6	0.100247	0.140815	370	0.712	0.9986
	2-7	0.394274	0.15097	370	2.612	0.1853
	2-8	0.108888	0.144748	370	0.752	0.9979
	2-9	0.235856	0.156478	370	1.207	0.8518
	3-4	0.450251	0.1461	370	3.082	0.0559
	3-5	0.121224	0.16048	370	0.755	0.9979
	3-6	0.239411	0.1414	370	1.693	0.7505
	3-7	0.533438	0.153039	370	3.486	**0.0159**
	3-8	0.248052	0.147484	370	1.682	0.7574
	3-9	0.37502	0.158811	370	2.361	0.3086
	4-5	-0.32903	0.151022	370	-2.179	0.4218
	4-6	-0.21084	0.136156	370	-1.549	0.8316
	4-7	0.083187	0.144019	370	0.578	0.9997
	4-8	-0.2022	0.137315	370	-1.473	0.8677
	4-9	-0.07523	0.151102	370	-0.498	0.9999
	5-6	0.118187	0.151399	370	0.721	0.9973
	5-7	0.412214	0.156746	370	0.630	0.1779
	5-8	0.126828	0.150639	370	0.842	0.9955
	5-9	0.253797	0.164391	370	1.544	0.8339
	6-7	0.294027	0.142155	370	2.068	0.4967
	6-8	0.008641	0.137538	370	0.063	1.0000
	6-9	0.135609	0.149432	370	0.908	0.9925
	7-8	-0.28539	0.140303	370	-2.034	0.5205
	7-9	-0.15842	0.154927	370	-1.023	0.9836
	8-9	0.126968	0.149683	370	0.848	0.9952

Table S3. Linear mixed effects model statistical output for ionocyte density and size in *Acanthochromis polyacanthus* and *Amphiprion melanopus* embryos. Bold text indicates significant *p*-values ($\alpha = 0.05$).

Metric	Species	Factor	D.F.	*F*-value	*p*-value
Ionocyte density	*Acanthochromis polyacanthus*	Intercept	1, 89	37.16515	**<0.0001**
		Age	7, 89	8.34830	**<0.0001**
		Tissue	1, 89	45.17837	**<0.0001**
		Age:Tissue	7, 89	3.57659	**0.002**
	Amphiprion melanopus	Intercept	1, 57	720.8790	**<0.0001**
		Age	5, 57	2.1497	**0.0725**
		Tissue	1, 57	49.5779	**<0.0001**
Ionocyte size	*Acanthochromis polyacanthus*	Intercept	1, 1121	3204.969	**<0.0001**
		Age	7, 1121	45.986	**<0.0001**
		Tissue	1, 1121	713.476	**<0.0001**
		Age:Tissue	7, 1121	19.042	**<0.0001**
	Amphiprion melanopus	Intercept	1, 810	9022.536	**<0.0001**
		Age	5, 810	33.621	**<0.0001**
		Tissue	1, 810	542.841	**<0.0001**
		Age:Tissue	5, 810	2.525	**0.028**

Table S4. Estimated marginal means statistical output for the comparison of ionocyte density across tissue and age in *Acanthochromis polyacanthus* embryos. Bold text indicates Pr(>|z|) values of significance ($\alpha = 0.05$).

Click here to download Table S4

Table S5. Estimated marginal means statistical output for the comparison of ionocyte size across tissue and age in *Acanthochromis polyacanthus* and *Amphiprion melanopus* embryos. Results are given on a log scale. Bold text indicates Pr(>|z|) values of significance ($\alpha = 0.05$).

Click here to download Table S5